Fuel Processing Technology, Volume 186, April 2019, pp. 8-17
DOI:10.1016/j.fuproc.2018.12.007

Combustion characteristics of lignite char in a fluidized bed under O_2/N_2, O_2/CO_2 and O_2/H_2O atmosphere

Lin Li[1], Lunbo Duan[1,*], Shuai Tong[1], Edward John Anthony[2]

1. *Key Laboratory of Energy Thermal Conversion and Control, Ministry of Education, School of Energy and Environment, Southeast University, Nanjing 210096, China*
2. *Centre for Combustion and CCS, School of Energy, Environment and Agrifood, Cranfield University, Cranfield, Bedfordshire MK43 0AL, UK*

**Corresponding author: Tel./fax: +86 (0) 25 83790147.*
E-mail address: duanlunbo@seu.edu.cn.

Abstract:

Oxy-fuel combustion, O_2/H_2O combustion has many advantages over O_2/CO_2 combustion, and has gradually gained more and more attention recently for carbon capture from coal-fired power plant. The unique physicochemical properties (thermal capacity, diffusivity, reactivity) of H_2O will definitely influence the coal combustion process. In this work, the combustion characteristics of lignite char were investigated in a fluidized bed combustor under O_2/N_2, O_2/CO_2 and O_2/H_2O atmospheres with different oxygen concentration (15 %-27 %) and bed temperature (837-937 ^oC). Results indicated that the average reaction rate ($r_{average}$) and the peak reaction rate (r_{peak}) of lignite char in O_2/H_2O atmosphere was lower than that in O_2/CO_2 atmospheres at low oxygen concentrations. However, as the oxygen concentration increased, the r_{peak} and $r_{average}$ in O_2/H_2O atmosphere was significantly improved and exceeded that in O_2/CO_2 atmosphere. The calculation of the activation energy based on the shrinking core model showed that the order of activation energy under different atmospheres is: O_2/CO_2 (28.96 kJ/mol) > O_2/H_2O (26.11 kJ/mol) > O_2/N_2 (23.31 kJ/mol). Furthermore, with the increase of the bed temperature, the active sites occupied by gasification agent were significantly increased, the active sites occupied by oxygen decreased correspondingly.

Keywords: O_2/H_2O combustion; fluidized bed; lignite char; gasification; activation energy.

1. Introduction

Oxy-fuel combustion technology (O_2/CO_2 combustion) is considered as a competitive technology for carbon capture from coal-fired power plants and has attracted extensive research in the past two decades [1]. Compared with conventional combustion, a mixture of pure O_2 and recycled flue gas is utilized as the oxidizer instead of air, resulting in more than 90% CO_2 concentration in exhaust flue gas after condensation, which is conducive to CO_2 separation [2, 3]. However, the low net efficiency and high cost is the biggest obstacle to the commercialization of this technology [4].

In recent years, a new technical route of oxy-fuel combustion which used steam rather than recycled flue gas to moderate the furnace temperature was proposed by Carlos [5], Seepana and Jayanti [6]. In oxy-steam combustion, the flue gas recycle system can be removed, further reducing the energy consumption and avoiding the air infiltration in the flue gas recycle lines. In addition, it also have many advantages over O_2/CO_2 combustion as follows [5, 6]: 1) the latent energy of water is much easier to recover owing to the enriched steam in the flue gas; 2) the size of major and auxiliary equipment of the system is smaller than those of O_2/CO_2

Published by Elsevier. This is the Author Accepted Manuscript issued with: Creative Commons Attribution Non-Commercial No Derivatives License (CC:BY:NC:ND 4.0).
The final published version (version of record) is available online at DOI:10.1016/j.fuproc.2018.12.007. Please refer to any applicable publisher terms of use.

combustion; 3) the formation of NO_x and SO_x can be decreased; 4) the power consumption of pump and fan is relatively low because the transmission medium is water rather than flue gas. Therefore, the oxy-steam combustion is identified as a promising next generation oxy-fuel combustion. When this technology is introduced to the fluidized bed combustion, it will bring more advantages such as realization of burning low-rank coal like lignite, uniform temperature distribution and inherent low SO_2/NO_x emission.

Up to now, only few researches on the oxy-steam combustion have been published, which were nearly all about pulverized coal (PC) furnaces. Jin et al. [7] investigated the process characteristics of oxy-steam power plant by steady-state process model in Aspen Plus. It was found that oxy-steam combustion exhibited better performance than O_2/CO_2 combustion on both thermodynamic and economic aspects. Salvador et al. [8] proposed burner design for oxy-steam combustion and conducted corresponding experiments in a 0.3 MW_{th} oxy-fuel combustor. It was concluded that oxy-steam combustion resulted in lower CO level, moderate NO_x, typical SO_x, and 5~10% boosting CO_2 concentration. Richards et al. [9] studied the residence time requirements and the equilibrium CO levels of oxy-steam combustion through the combination of experiments and simulations. The results showed that the residence time was 5~7 times greater and the equilibrium CO levels were higher for the O_2/CO_2 combustion when compared with O_2/H_2O combustion. Zou et al. [10-12] performed a series of experiments on the thermal gravimetric analyzer and the drop tube furnace to study ignition and combustion characteristics of PC in O_2/N_2 and O_2/H_2O atmospheres. The results showed that the ignition of PC in the O_2/H_2O atmospheres occurred sooner than that in the O_2/N_2 atmospheres at identical oxygen fractions. It can be attributed to the existence of the steam gasification reaction ($C+H_2O \rightarrow CO+H_2$) and the shift reaction ($CO+H_2O \rightarrow CO_2+H_2$) in H_2O atmosphere. However, fluidized bed (FB) combustion differs significantly from PC combustion in terms of hydrodynamics, reaction kinetics and heat transfer.

Existing research for FB combustion were mainly on O_2/CO_2 atmosphere rather than O_2/H_2O atmosphere. A 0.8 MW_{th} oxy-fuel CFB boiler was carried out by Tan et al. [13], achieving smooth transition between air-combustion and oxy-fuel combustion. Under stable oxy-fuel combustion condition, CO_2 concentrations can be reached to more than 90% (on a dry basis), while the reduction of the emissions of NO_x and SO_x can be observed at the same time. Similar conclusions were also obtained by Monica et al. [14] in a 30 MW_{th} oxy-CFB Boiler. Three kinds of fuel were burned in a 50 kW_{th} oxy-fuel CFB combustor with warm flue gas recycle has been reported by Duan et al. [15]. The results showed that an equivalent or higher carbon burnout can be realized with a slightly higher O_2 concentration (22.2%-23.4% for different fuels) in oxy-fuel combustion. Scala and Chirone [16, 17] studied the combustion characteristics of a single char particle in a FB reactor and found the Char-CO_2 gasification was the main reaction in O_2/CO_2 combustion. Additionally, a series of studies on combustion characteristics of single coal particle also have been performed in a FB under O_2/CO_2 atmosphere [18-21].

As referred above, there has been no work published on oxy-steam fluidized bed combustion of coal char, and the combustion mechanism has not been fully clarified for oxy-steam combustion. Consequently, the aim of the present work is to evaluate the combustion characteristics (such as the peak reaction rate, the burnout time and the average reaction rate) and kinetic characteristics in FB under O_2/H_2O atmospheres, and quantitatively analyzing the

effect of gasification on combustion process.

2. Experimental

2.1 Materials

On account of lignite is a commonly used coal for fluidized bed boiler, a lignite (Xiaolongtan lignite from China) was selected as the test coal in present work. The proximate and ultimate analysis are shown in Table 1.

The fuel particle size of circulate fluidized bed boiler is generally 0-13 mm. However, large coal particle combustion is significantly affected by diffusion, and too small particle is easily carried out of the furnace by fluidized gas. Therefore, in order to evaluate the combustion and kinetic characteristics of lignite char in fluidized bed, a relatively small particle size of test coal (1.25~1.5 mm) was selected to minimize the influence of diffusion control region in this paper. Before the test, the lignite need to be devolatilized in a fluidized bed reactor with N_2 atmosphere at 900 °C for 7 min, then the char particle with size range of about 1~1.2 mm were achieved.

Quartz sands (0.3-0.35 mm, 2560 kg/m^3) were used as the bed material with unexpanded bed height of 150 mm in the test, the corresponding minimum fluidization velocity (u_{mf}) was 0.042 m/s. The fluidized velocity (u_f) was set at 0.126 m/s (u_f/u_{mf} =3), corresponding the bubbling condition.

Table 1 Properties of the coal samples.

Fuel	Proximate analysis, wt% (as received)				Ultimate analysis, wt% (dry and ash-free basis)				
	Moisture	Volatile	Fixed carbon	Ash	C	H	O[a]	N	S
Lignite	16.17	35.53	39.18	9.12	67.11	4.23	25.07	1.45	2.14

[a] By difference

2.2 Experimental system

A lab-scale fluidized bed combustor was used in this study. The schematic diagram of the experimental system is shown in Fig. 1. The system mainly contained four parts: the gas and water supply line, the fluidized bed (FB) reactor, the temperature controlling system and the data acquisition system of flue gas.

The flow of O_2, N_2 and CO_2 from cylinders were controlled by three digital mass flowmeters, respectively. A high-precision syringe pump was used to control the injection rate of deionized water before heating in evaporator. Then the steam was mixed with O_2 or N_2 stream as the fluidization gas fed into the combustor. The FB reactor was made of quartz glass with inner diameter of 22 mm and length of 1200 mm, which included the preheating section with the length of 500 mm. The preheating section and the reaction section were heated by 1 kW and 5 kW electrical heaters, respectively. The furnace temperature was continuously controlled within ±5 °C deviation by a PID controller, which was verified by the measurement of a moving thermocouple. At the outlet of reactor, the flue gas was rapidly cooled and dried. Then the gas products were analyzed by the online Fourier transform infrared multi-component gas analyzer (with the resolution of 1ppm). In order to ensure that all kinds of gas products were in the optimum measuring range of gas analyzer, a certain amount (1.2 L for O_2/N_2 atmosphere, 1.8 L for O_2/CO_2 atmosphere and 2.5 L for O_2/H_2O atmosphere) of N_2 was used as a dilution gas and fed into the gas analyzer at the same time.

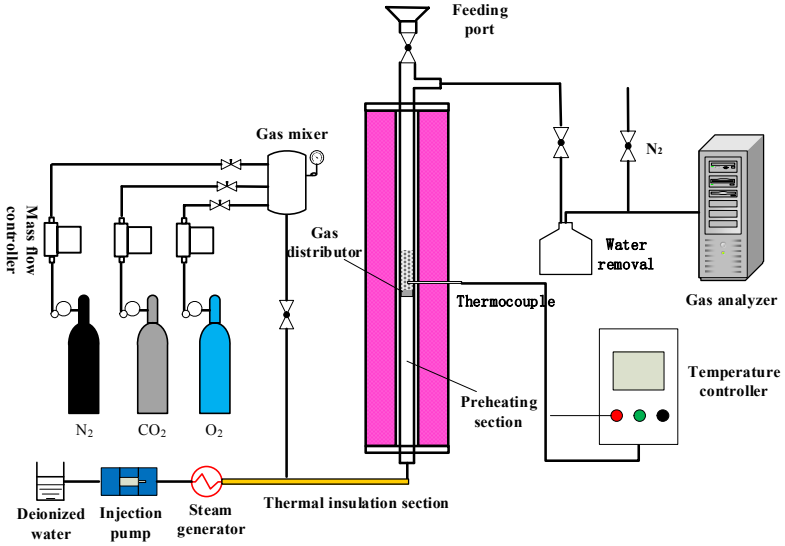

Fig. 1. The schematic diagram of experimental system.

2.3 Experimental procedure

After heating the FB combustor to the set temperature, the water and fluidizing gas were introduced into reactor. 200 mg of char samples were injected into the reactor after the fluidization condition reached a steady state. The tests were performed in O_2/N_2, O_2/CO_2, O_2/H_2O, N_2/CO_2 and N_2/H_2O atmospheres with different oxygen concentrations (0%, 15%, 21% and 27%) and bed temperatures (837 °C, 887 °C and 937 °C). The operating conditions are summarized in Table 2. Each test was repeated at least three times to guarantee the good repeatability. In fact, the results would be discarded and repeated if the carbon balance ratio error of the test exceeded ±10%.

Before experiments, water balance tests were carried out by comparing the amount of water injected in the pre-heater furnace (V_{in}) with the amount of condensate water in the outlet of reactor (V_{out}). For all the tests, water balance ratios (V_{out}/V_{in}) were more than 98% within 2 hours.

Table 2 Operating conditions used in tests.

Fuel	T_b (°C)	Atmosphere	O_2 or N_2 (%)
Lignite char	837, 887, 937	O_2/N_2, O_2/CO_2, O_2/H_2O	21 (O_2)
	887	O_2/N_2, O_2/CO_2, O_2/H_2O	15, 21, 27 (O_2)
	837, 887, 937	N_2/CO_2, N_2/H_2O	21 (N_2)
	887	N_2/CO_2, N_2/H_2O	15, 21, 27 (N_2)

2.4 Data treatment

It should be noted that only a small amount of CH_4 (less than 40 ppm) were measured in O_2/H_2O atmospheres, so only the CO and CO_2 were considered as the parameters in the carbon balance calculation. Fig. 2 shows the typical concentration profiles of CO and CO_2 for the combustion test under different atmosphere. In O_2/N_2 and O_2/CO_2 atmospheres, char combustion process can be described by three global reactions [17, 21]:

$$C + O_2 = CO_2 \qquad \Delta H = -394 \text{ kJ/mol} \tag{1}$$

$$C + CO_2 = 2CO \qquad \Delta H = +171 \text{ kJ/mol} \tag{2}$$

$$2CO + O_2 = 2CO_2 \qquad \Delta H = -283 \text{ kJ/mol} \tag{3}$$

However, char combustion in O_2/H_2O atmospheres will occur additional reactions [11, 21]:

$$C + H_2O = H_2 + CO \qquad \Delta H = +130 \text{ kJ/mol} \tag{4}$$

$$CO + H_2O = H_2 + CO_2 \qquad \Delta H = -40 \text{ kJ/mol} \tag{5}$$

$$2H_2 + O_2 = 2H_2O \qquad \Delta H = -242 \text{ kJ/mol} \tag{6}$$

The carbon conversion rate was calculated as following expression:

$$X = (W_{CO,i} + W_{CO2,i})/W_{C,\infty} \tag{7}$$

where X is the carbon conversion rate; $W_{CO,i}$ and $W_{CO2,i}$ represent the weight of carbon in CO and CO_2 generated in the reaction time from 0 to i, respectively; $W_{C,\infty}$ represents the weight of carbon generated during the whole reaction process. The amount of CO and CO_2 can be calculated as:

$$W_{CO,i} = \int_0^i M_C \cdot C_{CO} \cdot Q/22.4 \cdot dt \tag{8}$$

$$W_{CO2,i} = \int_0^i M_C \cdot (C_{CO2} - C_{CO2,0}) \cdot Q/22.4 \cdot dt \tag{9}$$

where M_C is the carbon molecular weight; t is the reaction time, C_{CO} and C_{CO2} represent the gas concentration of CO and CO_2 measured by the gas analyzer; C_{CO2} is the CO_2 concentration at the inlet of reactor; Q is the flow rate at the outlet of reactor.

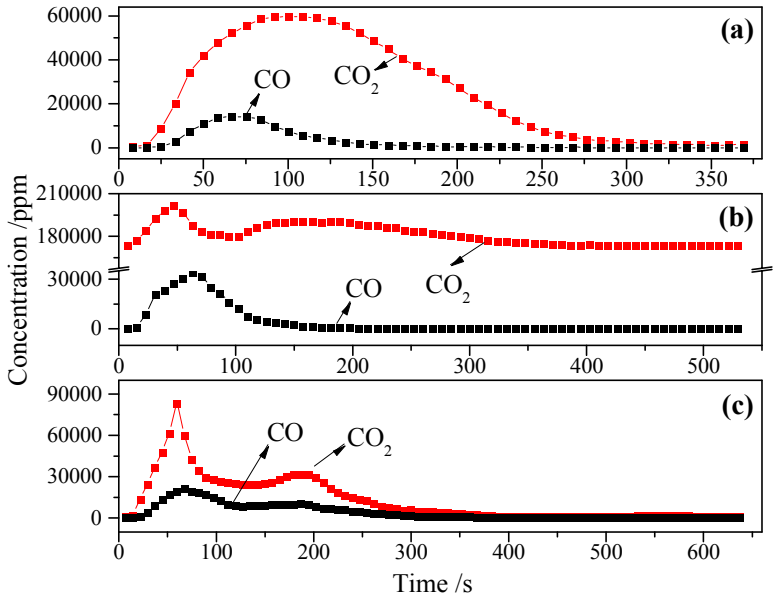

Fig. 2 Typical CO and CO_2 measured outlet profiles during char combustion tests: (a) O_2/N_2 combustion (T = 937 °C, 21% O_2/79% N_2); (b) O_2/CO_2 combustion (T = 937 °C, 21% O_2/79% CO_2); (c) O_2/H_2O combustion (T = 937 °C, 21% O_2/79% H_2O).

2.5 Reliability analysis of the measurements

The reliability of the measurements was examined by carbon balance ratio which can be calculated by

$$\text{Carbon balance ratio} = \frac{W_{co,\infty} + W_{co2,\infty}}{W_{c,0}} \times 100\% \tag{10}$$

where the $W_{C,0}$ is the carbon content of the sample particles. The carbon balance ratio of this investigation are shown in Fig. 3. It indicated that the carbon balance ratio of all tests were in range of 90% - 110%, which proved that the measurement was accurate and reliable.

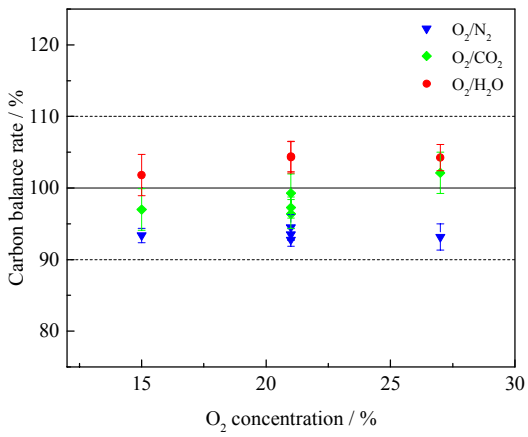

Fig. 3. Carbon balance rate in different conditions.

3. Treatment method

3.1 Kinetic approach

The combustion reaction rate was described as

$$dX/dt = k \cdot f(X) \tag{11}$$

where $f(X)$ is the reaction model; k is the reaction rate constant, which was calculated by Arrhenius equation

$$k = A\exp(-E/RT) \tag{12}$$

where A is pre-exponential factor; E is the activation energy; T is the reaction temperature; R is the molar gas constant, 8.314 J/(mol·k). Rearranging the Eq. (11)

$$\frac{1}{f(X)}\mathrm{d}X = k\mathrm{d}t \tag{13}$$

The gasification and combustion reaction kinetic models of coal is random and complex among the numerous kinetic models. In this work, the shrinking core model was adopted to calculate kinetic parameters of char combustion, which have been proven by many researchers to be a suitable model for coal combustion and gasification research [22-24]. It was given by

$$\mathrm{G}(X) = 1-(1-X)^{1/3} \tag{14}$$

where $G(X)$ is mechanism function model. Combining Eq. (13) with Eq. (14)

$$\mathrm{G(X)} = 1-(1-X)^{\frac{1}{3}} = \int_0^X \frac{1}{\mathrm{f}(X)} dX = \int_0^t k dt = kt \tag{15}$$

The k at different conditions could be calculated by the slope of Eq. (15). Then applying the natural logarithm to Eq. (12),

$$\ln k = \ln A - E/RT \tag{16}$$

The E and A were calculated by the slope ($-E/R$) and the intercept ($\ln A$) of Eq. (16).

3.2 Calculation of carbon consumption rate

Generally, the differences of char combustion in O_2/CO_2, O_2/H_2O and O_2/N_2 atmospheres are mainly brought by two aspects: (1) Gasification. The gasification reaction of char (such as Eq. (1) and Eq. (4)) which cannot be neglected in the oxygen-fuel combustion (O_2/CO_2 and O_2/H_2O); (2) Diffusivity of oxygen. The diffusivity of O_2, CO_2 and H_2O in the binary gaseous mixture are shown in Fig. 4. It is clear that the diffusivity of O_2 in O_2/H_2O atmospheres is over 20% higher than that in O_2/N_2 atmospheres, and the diffusion rate of O_2 in O_2/CO_2 atmosphere is the lowest.

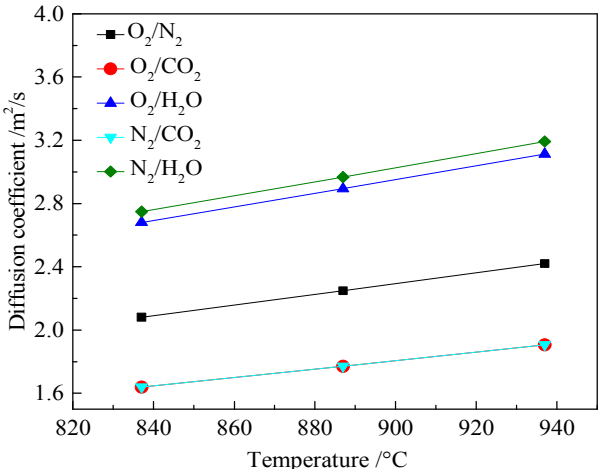

Fig. 4. Diffusion rate in different atmospheres.

The simulated carbon consumption rate (v_{cal}) could be calculated by accumulation of carbon consumption rate of oxidation and gasification reactions. It needs to be pointed out that the amount of quartz sands was much greater than that of test char, and the particle size of the char was small, so good heat transfer between char and bed material ensured that their temperatures are almost the same. The theory was also supported by Roy and Bhattacharya [21], who carried out experiments and simulation studies on the single coal char combustion with different particle sizes (≥1 mm) under oxy-fuel fluidized bed condition, and found that when the size of char was 1 mm, the error caused by the assumption of equal particle and bed temperatures was negligible. The v_{cal} can be expressed as

$$v_{cal}=v_{oxi}+v_{gas} \tag{17}$$

where v_{oxi} and v_{gas} are the reaction rate of oxidation and gasification, respectively. The v_{oxi} and v_{gas} were obtained by testing the char reaction rate in O_2/N_2, N_2/CO_2 and N_2/H_2O atmospheres at the same partial pressure of reactant. Besides, the C-O_2 oxidation is also affected by oxygen diffusion in the boundary layer [25], so the reaction rate of oxidation in O_2/CO_2 and O_2/H_2O atmospheres can be calculated by

$$v_{oxi,O2/CO2}= v_{O2/N2}\cdot D_{O2/CO2}/D_{O2/N2} \tag{18}$$

$$v_{oxi,O2/H2O}= v_{O2/N2}\cdot D_{O2/H2O}/D_{O2/N2} \tag{19}$$

where $v_{oxi,O2/N2}$, $v_{oxi,O2/CO2}$, $v_{oxi,O2/H2O}$ represent the reaction rate of oxidation in O_2/N_2, O_2/CO_2 and O_2/H_2O atmospheres, respectively; $D_{O2/N2}$, $D_{O2/CO2}$ and $D_{O2/H2O}$ represent the diffusivity of oxygen in O_2/N_2, O_2/CO_2 and O_2/H_2O atmospheres, respectively. The reaction rate of gasification in O_2/CO_2 and O_2/H_2O atmospheres can be given by

$$v_{gas,O2/CO2}= v_{N2/CO2}\cdot D_{O2/CO2}/D_{N2/CO2} \tag{20}$$

$$v_{gas,O2/H2O}= v_{N2/H2O}\cdot D_{O2/CO2}/D_{N2/H2O} \tag{21}$$

where $v_{gas,N2/H2O}$, $v_{gas,N2/CO2}$, $v_{gas,O2/CO2}$ and $v_{O2/H2O}$ are represented the reaction rate of gasification in N_2/H_2O, N_2/CO_2, O_2/CO_2 and O_2/H_2O atmospheres, respectively; $D_{N2/CO2}$ and $D_{N2/H2O}$ represent the diffusivity of CO_2 or H_2O in N_2/CO_2 and N_2/H_2O atmospheres, respectively.

The summation of carbon consumption rates of oxidation and gasification was also compared with the carbon consumption rate from experimental conditions (v_{exp}) of O_2/CO_2 and O_2/H_2O atmospheres. The relationship between gasification and oxidization in char combustion process can be expressed as follows:

(I) Mutual Promotion: $v_{cal} < v_{exp}$;

(II) Shared active site: $v_{cal} = v_{exp}$;

(III) Partial Shared activity site: $v_{oxi} < v_{exp} < v_{cal}$;

(IV) Mutual competition: $v_{exp} \leq v_{oxi}$.

4 Results and discussion

4.1 Carbon consumption rate of char

The reaction rate and carbon conversion rate of lignite char with various oxygen inlet concentration under N_2, CO_2 and H_2O atmospheres at different bed temperature are plotted in Fig. 5 and Fig. 6. The general char combustion behavior in O_2/N_2 atmosphere was obtained: After feeding the char sample into the reactor, it was ignited immediately and the reaction rate was reached the peak rapidly. As the char was continuously consumed, the reaction rate gradually decreased until the reaction was stopped. Interestingly, there were two peaks in reaction rate curves in O_2/CO_2 and O_2/H_2O atmospheres while there was only one peak in O_2/N_2 atmosphere, and the peak of reaction rate in O_2/H_2O atmosphere were larger than that in O_2/CO_2 atmosphere at the same oxygen concentration. Furthermore, it could be found that the second peak of reaction rate increased with the steam concentration in O_2/H_2O atmosphere, as shown in Fig. 5c. This may be caused by the existence of gasification in CO_2 and H_2O environments. With the advancement of reaction, the pore structure and specific surface area of char would be greatly strengthened, and further promoting the gasification reaction. Due to the C-H_2O reaction is stronger than C-CO_2 reaction at the same condition [26], the peak reaction rate in O_2/H_2O atmosphere were larger than that in O_2/CO_2 atmosphere.

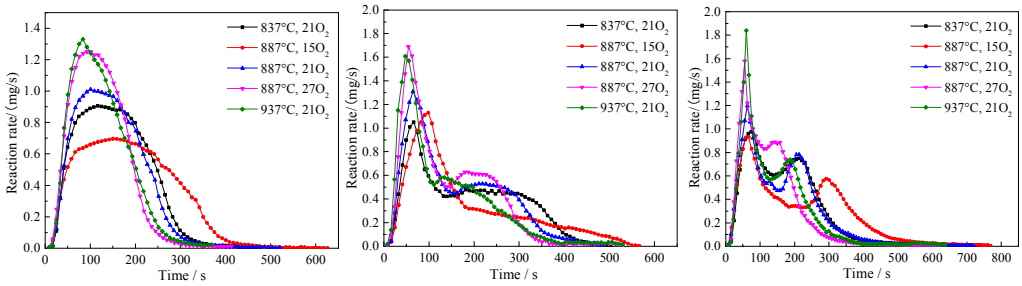

（a）O_2/N_2 (b) O_2/CO_2 (c) O_2/H_2O

Fig. 5. Reaction rate in different conditions.

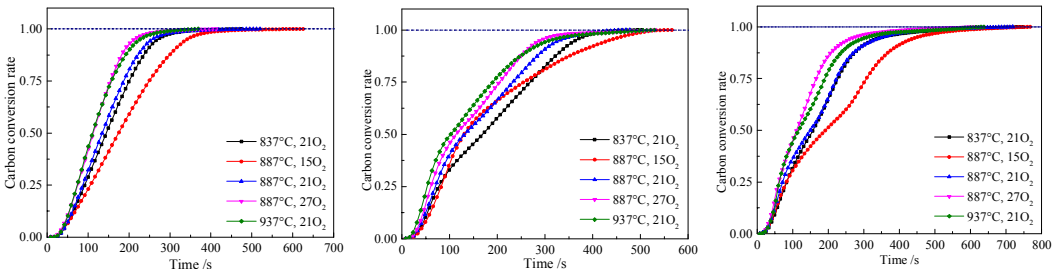

（a）O_2/N_2 (b) O_2/CO_2 (c) O_2/H_2O

Fig. 6. Carbon conversion rate in different conditions.

4.2 Char combustion characteristics

Fig. 7 shows the peak reaction rate (r_{peak}), burnout time (t_b) and average reaction rate ($r_{average}$) with 21% of oxygen concentration under N_2, CO_2 and H_2O atmospheres at different bed temperature. It can be seen from Fig. 7 that with the increase of temperature, the t_b decreased, and r_{peak} and $r_{average}$ increased. This result can be expected, because the gasification and oxidation reactions are enhanced at high temperatures. In the same oxygen concentration

and bed temperature, the burnout time sequence was: $O_2/N_2<O_2/H_2O<O_2/CO_2$. The reason can be attributed to the endothermic nature of the gasification, which will reduce the temperature of char particles, thus reducing the reactivity of char. In addition, the diffusion of O_2 in steam (2.68 m^2/s in 837°C) is 1.63 times larger than that in CO_2 atmosphere (1.64 m^2/s in 837 °C), which will greatly promote the oxidation of char particle. So the t_b in O_2/H_2O atmosphere was shorter than that in O_2/CO_2 atmosphere.

The r_{peak}, t_b and $r_{average}$ with different oxygen concentration under N_2, CO_2 and H_2O atmospheres at 887 °C are plotted in Fig. 8. It can be seen that the effect of the oxygen concentration on char combustion characteristics is similar to that of the bed temperature, while the effect of changing oxygen concentration was more significant. The t_b of char particle in O_2/H_2O atmosphere was longer than that in O_2/CO_2 and O_2/N_2 atmospheres at low oxygen concentration. However, as the oxygen concentration increases, the t_b in O_2/H_2O atmosphere was significantly improved and exceeded that in O_2/CO_2 atmosphere. There are two kinds of effects of steam on the char combustion in O_2/H_2O atmospheres: 1) the steam-char gasification reaction (Eq. (4)). 2) the steam shift reaction[11](Eq. (5)). At low oxygen concentration, higher partial pressure of steam results in a stronger gasification reaction, which will significantly reduce the temperature and reactivity of char particles. With the increase of oxygen concentration, the gasification reaction is weakened and oxidation reaction is strengthened. Furthermore, the steam shift reaction is an exothermic reaction, which is benefit to the char combustion. Similar conclusions were also obtained by Zou et al. [11], who studied the ignition behavior of pulverized coal in a drop tube furnace under O_2/N_2 and O_2/H_2O atmospheres.

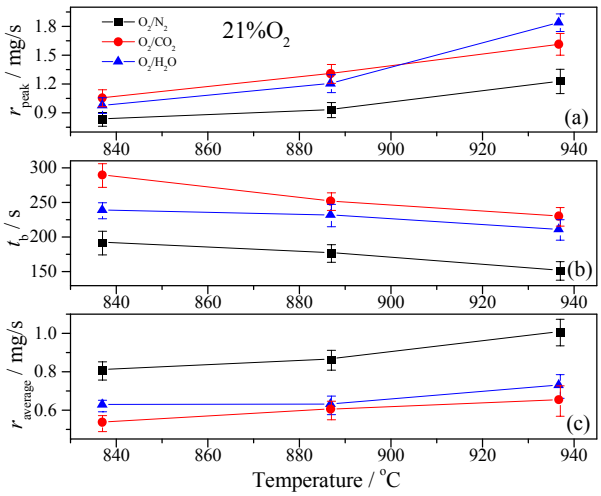

Fig. 7 The r_{peak}, t_b and $r_{average}$ with 21% of oxygen concentration under N_2, CO_2 and H_2O atmospheres at different bed temperature.

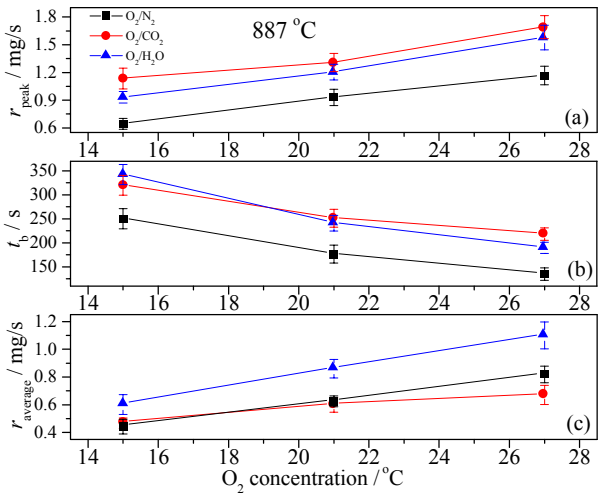

Fig. 8The r_{peak}, t_b and $r_{average}$ with different oxygen concentration under N_2, CO_2 and H_2O atmospheres at the bed temperature of 887 °C.

4.3 Analyses of combustion reaction kinetics

According to Eq. (15), the integral format of the reaction model *G(X)* should be proportional to the reaction time at a constant temperature in theory. Combined with the cumulative carbon conversion rate curve in Fig. 6, in order to minimize the influence of char heating, char mixing and diffusion control region on reaction kinetics analysis in the combustion process, the carbon conversion in the range of 0.1~0.85 was chosen to analyze reaction kinetics in this work. Fig. 9 displayed the modeling and experiment results of char combustion. It is indicated that the shrinking core model fitted the experiment results well in different conditions.

According to Eq. (16), the activation energy (*E*) and pre-exponential factor (*A*) of lignite char combustion were obtained by linear fitting and the results are shown in Fig. 10. The calculation results of the kinetics parameters are given in Table 5. The results illustrated that the order of activation energy under different atmospheres is: O_2/CO_2>O_2/H_2O>O_2/N_2. It is widely accepted that the larger activation energy means the worse reactivity of reactants. So the lignite char had the best reactivity in O_2/N_2 atmosphere and the worst reactivity in O_2/CO_2 atmosphere. It may be attributed that the char was oxidized and gasified simultaneously in O_2/CO_2 and O_2/H_2O atmospheres, whereas only the oxidation reaction was occurred in O_2/N_2 atmosphere. There is a competitive mechanism between the oxidation and gasification reaction [27], and the heat absorption of gasification reduces the char particle temperature and inhibits the activity of oxidation reaction.

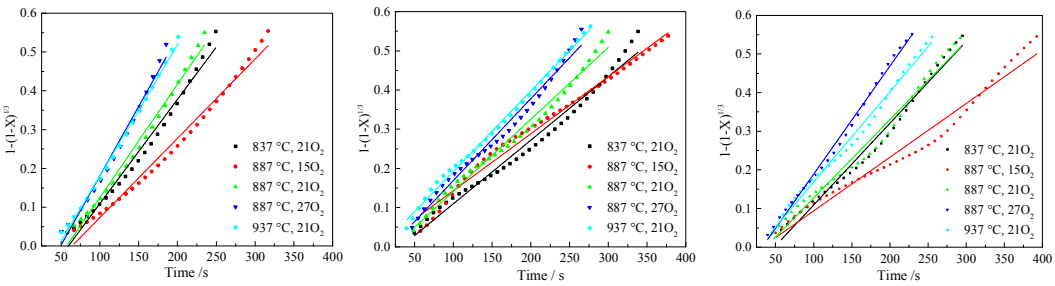

（a）O_2/N_2 (b) O_2/CO_2 (c) O_2/H_2O

Fig. 9 Fitting results of char combustion using shrinking core model in different conditions.

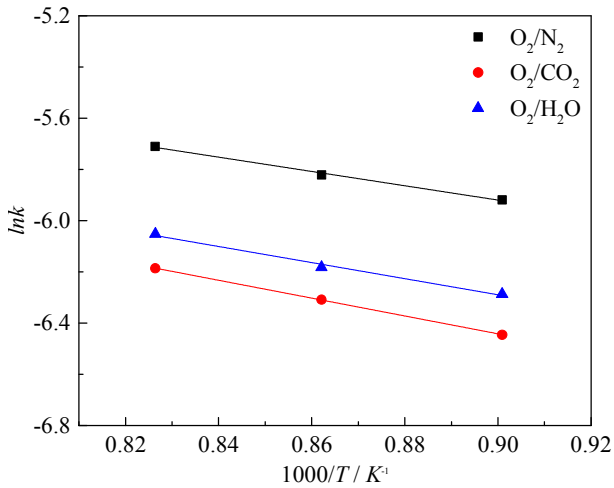

Fig. 10 Fitting results between reaction rate and temperature.

Table 3 Kinetics parameters of lignite char combustion.

Atmosphere	E (kJ/mol)	A (s^{-1})	R^2
21%O_2/79%N_2	23.31	0.0332	0.992
21%O_2/79%CO_2	28.96	0.0366	0.999
21%O_2/79%H_2O	26.11	0.0313	0.985

4.4 Quantitative analysis of gasification and oxidation reaction

4.4.1 Effect of CO_2 and H_2O in feed gas

The variation of average carbon reaction rate versus bed temperature and oxygen concentrations in O_2/CO_2 and O_2/H_2O atmospheres are plotted in Fig. 11 and Fig. 12. It is obviously that the calculated total carbon conversion rates were significantly larger than that of the experimental results, and the experimental carbon conversion rates were even lower than the calculated carbon conversion rates of oxidation. It can be concluded that competition reaction exists between the gasification and oxidation reaction in the char combustion process under O_2/CO_2 and O_2/H_2O atmospheres. Fig. 11 also shown that the difference between calculated results and experimental results increase with the bed temperature. This is because the reaction rate of gasification and oxidation increased significantly with the increase of bed temperature, which would cause more intense competition between them. Otherwise, the partial pressure of CO_2 and H_2O decreased with the increase of oxygen concentration, as a consequence the gasification reaction rate slightly decreased at high oxygen concentration, and the effect of gasification on the combustion progress reduced. The detailed quantitative analysis of the proportions of gasification and oxidation reaction in char combustion progress will be shown in 4.4.2.

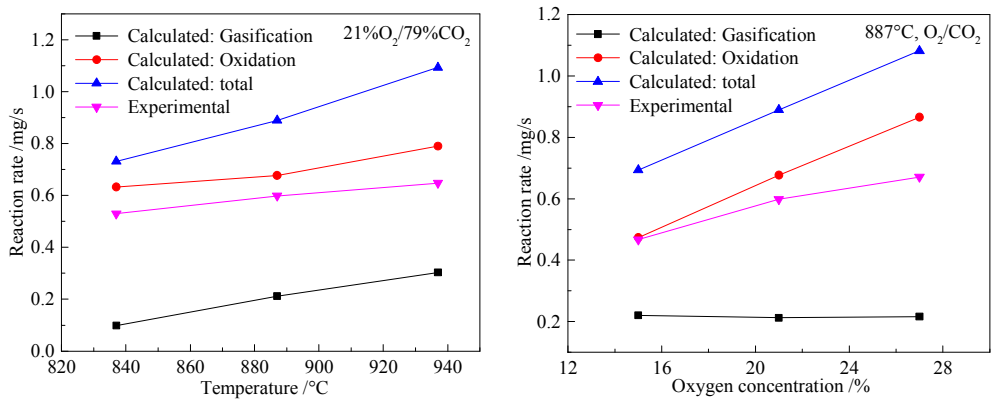

(a) 21%O_2/79%CO_2 (b) 887 °C

Fig. 11 Experimental and calculated average carbon conversion rate in different conditions under O_2/CO_2 atmosphere.

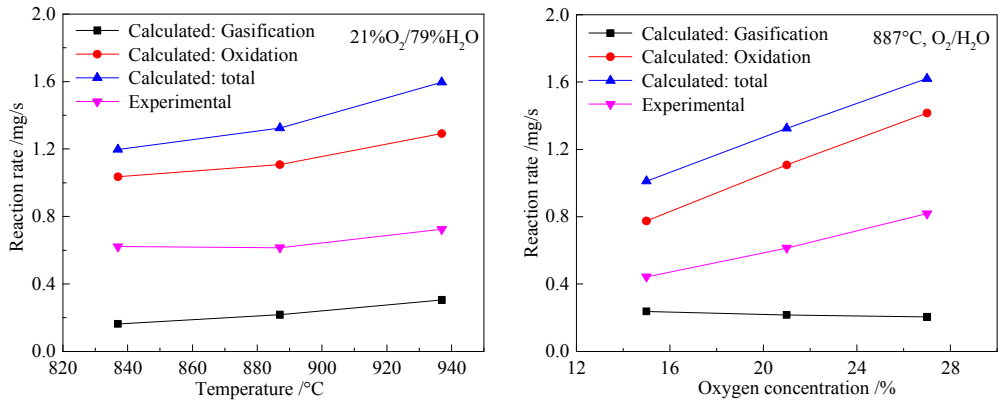

(a) 21%O_2/79%H_2O (b) 887 °C

Fig. 12 Experimental and calculated average carbon conversion rate in different conditions under O_2/H_2O atmosphere.

4.4.2 Quantitative analysis

The average combustion rate of char in O_2/CO_2 and O_2/H_2O atmospheres can be expressed as:

$$v_{O2/CO2} = a \cdot v_{N2/CO2} + b \cdot v_{O2/N2} \tag{22}$$

$$v_{O2/H2O} = a \cdot v_{N2/H2O} + b \cdot v_{O2/N2} \tag{23}$$

$$a+b=1 \tag{24}$$

where the a and b are represented the active sites occupied by gasification agent (CO_2 or H_2O) and oxidant (O_2) on the char surface in the combustion progress, respectively. The variation of a and b versus bed temperature and oxygen concentrations in O_2/CO_2 and O_2/H_2O atmospheres are showed in Table 4, and the corresponding reaction rate are displayed in Table 5. It can be found that the reaction rate of gasification and oxidation both increased with the increase of bed temperature, this is attributed to the higher reactivity of char at high temperature. At the same oxygen concentration, the active sites occupied by gasification agent significantly increased with bed temperature, and the active sites occupied by oxygen decreased correspondingly. The phenomenon indicated that when the char was burned in O_2/CO_2 or O_2/H_2O atmosphere, the inhibitory effect of the gasification reaction on the oxidation reaction was strengthened as the increase of temperature. Moreover, it is noticed clearly that the proportion of gasification reaction in O_2/H_2O atmospheres were higher than that in O_2/CO_2

atmospheres. This is due to the activity of C-H_2O reaction is better than that of C-CO_2 reaction. Interestingly, the v_{oxi} and (v_{oxi}+v_{gas}) in O_2/H_2O atmosphere were all lower than that in O_2/CO_2 atmosphere at low oxygen concentration. However, with the increase of oxygen concentration, the v_{oxi} and (v_{oxi}+v_{gas}) in O_2/H_2O atmosphere were remarkably strengthened and exceeded that in O_2/CO_2 atmosphere. The results indicated that the char combustion rate in O_2/H_2O atmosphere shows greater advantages at high oxygen concentrations than that in O_2/CO_2 atmosphere.

Table 4. Values of the *a* and *b*

	837°C	887°C	887°C	887°C	937°C
O_2/CO_2	21%O_2	15%O_2	21%O_2	27%O_2	21%O_2
a	0.193	0.065	0.211	0.300	0.293
b	0.807	0.935	0.789	0.700	0.707
O_2/H_2O	21%O_2	15%O_2	21%O_2	27%O_2	21%O_2
a	0.474	0.617	0.554	0.493	0.575
b	0.526	0.383	0.446	0.507	0.425

Table 5. Gasification and oxidation reaction rates during char combustion

	837°C	887°C	887°C	887°C	937°C
O_2/CO_2	21%O_2	15%O_2	21%O_2	27%O_2	21%O_2
V_{gas}	0.019	0.014	0.045	0.065	0.089
v_{oxi}	0.511	0.443	0.534	0.606	0.559
O_2/H_2O	21%O_2	15%O_2	21%O_2	27%O_2	21%O_2
V_{gas}	0.077	0.147	0.120	0.101	0.175
v_{oxi}	0.580	0.297	0.494	0.718	0.549

5 Conclusion

The goals of this study are to obtain the combustion characteristics of lignite char in a fluidized bed under O_2/H_2O, O_2/CO_2 and O_2/N_2 atmospheres. The main conclusions can be drawn as follows：

(1) With the increase of temperature and O_2 concentration, the similar combustion characteristics of lignite char were exhibited in O_2/H_2O, O_2/CO_2 and O_2/N_2 atmospheres (the t_b decreased, while r_{peak} and $r_{average}$ increased).

(2) At low oxygen concentration, the combustion characteristics of lignite char in O_2/H_2O atmosphere was worse than that in O_2/CO_2 and O_2/N_2 atmospheres; however, as the oxygen concentration increases, the combustion characteristics in O_2/H_2O atmosphere was significantly improved and exceeds that in O_2/CO_2 atmosphere.

(3) The calculation results showed that the relationship among activation energy under different atmospheres is: O_2/CO_2 (28.96 kJ/mol) > O_2/H_2O (26.11 kJ/mol) > O_2/N_2 (23.31 kJ/mol).

(4) The active sites occupied by gasification agent significantly increased as the bed temperature increases, and the competitive effect of gasification on oxidation is enhanced.

Acknowledgements

This work was financially supported by the National Natural Science Foundation of China (NO. 51776039).

References

[1] Buhre B J P, Elliott L K, Sheng C D, et al. Oxy-fuel combustion technology for coal-fired power generation[J]. Progress in Energy & Combustion Science, 2005, 31(4): 283-307.

[2] Wall T F. Combustion processes for carbon capture [J]. Proceedings of the Combustion Institute, 2007, 31(1): 31-47.

[3] Toftegaard M B, Brix J, Jensen P A, et al. Oxy-fuel combustion of solid fuels [J]. Progress in Energy & Combustion Science, 2010, 36(5): 581-625.

[4] Lasek J A, Janusz M, Zuwała J, et al. Oxy-fuel combustion of selected solid fuels under atmospheric and elevated pressures [J]. Energy, 2013, 62(6): 105-112.

[5] Carlos S. Modeling design and pilot-scale experiments of CANMET'S advanced oxy-fuel/steam burner. USA: International Oxy-Combustion Research Network; 2007.

[6] Seepana S, Jayanti S. Steam-moderated oxy-fuel combustion [J]. Energy Conversion & Management, 2010, 51(10): 1981-1988.

[7] Jin B, Zhao H, Zou C, et al. Comprehensive investigation of process characteristics for oxy-steam combustion power plants[J]. Energy Conversion & Management, 2015, 99: 92-101.

[8] Salvador C, Mitrovic M, Kourash K. Novel oxy-steam burner for zero-emission power plants. http://www.ieaghg.org/docs/oxyfuel/OCC1/Session%206_C/2_NOVEL%20OXY-TEAM%20BURNER%20FOR%20ZERO-EMISSION%20POWER%20PLANTS.pdf >.

[9] Richards G A, Casleton K H, Chorpening B T. CO_2 and H_2O diluted oxy-fuel combustion for zero-emission power [J]. Institute of Mechanical Engineers Part A Power & Energy, 2005, 219(2): 121-126.

[10] Lei C, Zou C, Yang L, et al. Numerical and experimental studies on the ignition of pulverized coal in O_2/H_2O atmospheres[J]. Fuel, 2015, 139: 198-205.

[11] Zou C, Cai L, Wu D, et al. Ignition behaviors of pulverized coal particles in O_2/N_2, and O_2/H_2O mixtures in a drop tube furnace using flame monitoring techniques [J]. Proceedings of the Combustion Institute, 2015, 35(3): 3629-3636.

[12] Zou C, Zhang L, Cao S, et al. A study of combustion characteristics of pulverized coal in O_2/H_2O atmosphere [J]. Fuel, 2014, 115: 312-320.

[13] Tan Y, Jia L, Wu Y, et al. Experiences and results on a 0.8 MW_{th} oxy-fuel operation pilot-scale circulating fluidized bed [J]. Applied Energy, 2012, 92(4): 343-347.

[14] Monica Lupion, Iñaki Alvarez, Pedro Otero, et al. 30 MW_{th} CIUDEN Oxy-CFB Boiler-First Experiences [J]. Energy Procedia, 2013, 37: 6179-6188.

[15] Duan L, Sun H, Zhao C, et al. Coal combustion characteristics on an oxy-fuel circulating fluidized bed combustor with warm flue gas recycle [J]. Fuel, 2014, 127(2): 47-51.

[16] Scala F, Chirone R. Combustion of Single Coal Char Particles under Fluidized Bed Oxyfiring Conditions [J]. Industrial & Engineering Chemistry Research, 2009, 49(21):11029-11036.

[17] Scala F, Chirone R. Fluidized bed combustion of single coal char particles at high CO_2, concentration [J]. Chemical Engineering Journal, 2010, 165(3): 902-906.

[18] Bu C, Bo L, Chen X, et al. Devolatilization of a single fuel particle in a fluidized bed under oxy-combustion conditions. Part A: Experimental results [J]. Combustion & Flame, 2015, 162(3): 797-808.

[19] Bu C, Bo L, Chen X, et al. Devolatilization of a single fuel particle in a fluidized bed under oxy-combustion conditions. Part B: Modeling and comparison with measurements [J]. Combustion & Flame, 2014, 162(3): 809-818.

[20] Bu C, Pallarès D, Chen X, et al. Oxy-fuel combustion of a single fuel particle in a fluidized bed: char combustion characteristics, an experimental study [J]. Chemical Engineering Journal, 2016, 287(3): 649-656.

[21] Roy B, Bhattacharya S. Combustion of single char particles from Victorian brown coal under oxy-fuel fluidized bed conditions [J]. Fuel, 2016, 165: 477-483.

[22] Sadhukhan A K, Gupta P, Saha R K. Analysis of the dynamics of coal char combustion with ignition and extinction phenomena: Shrinking core model [J]. International Journal of Chemical Kinetics, 2008, 40(9): 569-582.

[23] Zhang L, Huang J, Fang Y, et al. Gasification Reactivity and Kinetics of Typical Chinese Anthracite Chars with Steam and CO_2 [J]. Energy & Fuels, 2006, 20(3): 1201-1210.

[24] Chen C, Wang J, Liu W, et al. Effect of pyrolysis conditions on the char gasification with mixtures of CO_2, and H_2O [J]. Proceedings of the Combustion Institute, 2013, 34(2): 2453-2460.

[25] Wang W, Bu C, Gómez–Barea A, et al. O_2/CO_2 and O_2/N_2 combustion of bituminous char particles in a bubbling fluidized bed under simulated combustor conditions [J]. Chemical Engineering Journal, 2018, 336: 74-81.

[26] Roberts D G, Harris D J. Char gasification in mixtures of CO_2 and H_2O: Competition and inhibition [J]. Fuel, 2007, 86(17): 2672-2678.

[27] Senneca O, Cortese L. Kinetics of coal oxy-combustion by means of different experimental techniques [J]. Fuel, 2012, 102: 751-759.

Cranfield University

CERES Research Repository **https://dspace.lib.cranfield.ac.uk/**

School of Water, Energy and Environment (SWEE) Staff publications (SWEE)

Combustion characteristics of lignite char in a fluidized bed under O2/N2, O2/CO2 and O2/H2O atmospheres

Li, Lin

2018-12-21

Attribution-NonCommercial-NoDerivatives 4.0 International

Li L, Duan L, Tong S, Anthony EJ. Combustion characteristics of lignite char in a fluidized bed under O2/N2, O2/CO2 and O2/H2O atmospheres. Fuel Processing Technology, Volume 186, April 2019, pp. 8-17

https://doi.org/10.1016/j.fuproc.2018.12.007

Downloaded from CERES Research Repository, Cranfield University